



---

RESEARCH ARTICLE

---

INVESTIGATION OF TAUTOMERIC STRUCTURES OF 6-AZA-2-THIOURACIL-5-CARBOXYLIC ACID USING VIBRATIONAL SPECTROSCOPY ALONG WITH DFT THEORETICAL METHOD

Gökhan DİKMEN \* 

Central Research Laboratory Research and Application Center (ARUM), Eskişehir Osmangazi University, Eskişehir, 26040, Turkey

ABSTRACT

Molecular structure, tautomeric forms, vibrational modes, optic and electronic properties of 6-Aza-2-thiouracil-5-carboxylic acid (6A2T5CA) molecule were characterized by FT-IR, Raman, UV-VIS spectral methods and DFT method. The experimental results show that FT-IR and Raman spectroscopic methods could be used to determine the different tautomeric forms of 6A2T5CA molecule clearly. Although the title molecule has different tautomeric forms such as oxo and hydroxyl because of inter molecular interactions, it also has other tautomeric forms, due to intra molecular interaction of functional groups within the molecule. In particular, such structures change between each other depending on the solvent medium. Differences in some vibrational bands were observed in IR and Raman spectra. These differences were observed especially in N-H and O-H functional groups. In addition, vibrational modes, optimized structures, energy values, electronic transitions and HOMO-LUMO energy values of tautomeric forms were calculated using B3LYP/6-311G(2d,2p) level of theory. Experimentally obtained results were compared with theoretically obtained results and it was indicated that there was a good agreement with each other. It was also observed that the molecule has a different tautomeric form when it was dissolved in ethanol however, the molecule has another tautomeric form when it was dissolved in water.

**Keywords:** 6-Aza-2-thiouracil-5-carboxylic acid, DFT, FT-IR, Raman, Tautomeric forms

---

1. INTRODUCTION

Thiouracil, derived from uracil, is one of the four RNA bases. Although, thiouracils are uracil derivatives, when uracils are replaced with thiouracils, problems are observed in the translation of genetic information. Moreover, thiouracils and their derivative molecules have been used in a lot of areas such as antithyroid, anticancer, anti-HIV and heart disease treatments [1-3]. Theoretical and experimental investigations of thiouracil derivative molecules have been studied because of their various biological activities [4-6]. 2-thiouracil comprises an important derivative of pyrimidines. It is used as a cross-linking agent in RNA transcriptional regulation [7, 8]. Geometric parameters, vibrational properties of uracil and its thio-derivatives were carried out by IR, Raman spectra and DFT [9]. 2-thio-6-azauracil, 4-thio-6-azauracil and 2,4- dithio-6-azauracil molecules have been examined by ab initio quantum chemical calculations [10]. 6-Azauracil has been used as antitumor drug [11]. 2-Thio-6-azauridine has been used as an active molecule against LI210 leukemia cells [12] Vibrational characterization of 2-thiouracil molecule using FT-IR and Raman spectroscopic method was performed in previously study [13]. Vibrational modes of uracil molecule were made using Ab initio calculations by Nishimura et al. [14]. In another study, the theoretical characterization of the 2-thiouracil molecule with DFT has been made [15]. The 4-thiouracil molecule similar to 2-thiouracil has been characterized using various spectroscopic methods [16] and this molecule theoretically characterized by ab initio and DFT [17, 18]. It has been observed that obtained the theoretical and experimental data are in agreement with each other. Since thiouracil molecule derivative molecules are biologically active molecules, theoretical and experimental characterization studies of these molecules are still continuing in the literature. Therefore,

experimental and theoretical characterization of 6-aza-2-thiouracil-5-carboxylic acid (6A2T5CA) molecule, which is a thiouracil derivative, has been done in this study.

FT-IR and Raman spectroscopies have been used in the determination of structural characterization of molecular systems. Moreover, DFT calculations have been used along with vibrational methods. DFT is a reliable method in the determination of physical and chemical properties of the targeted molecules [19-22].

In present study, the most stable isomer of 6-aza-2-thiouracil-5-carboxylic acid (6A2T5CA) was studied based on the DFT results. Some geometrical parameters, vibrational wavenumbers of 6A2T5CA were computed at B3LYP/6-311G(2d, 2p) basis set. Moreover, experimentally obtained data were compared with theoretically obtained data. All of the results of the both theoretical and experimental studies were reported.

## **2. MATERIALS AND METHODS**

6A2T5CA (95%) was bought from Sigma Aldrich. FT-IR spectrum was measured by Perkin Elmer Spectrum Two with preparing the KBr pellets. Raman spectrum of 6A2T5CA was collected by Renishaw Invia Raman spectrometer. Raman spectra were taken using 532 nm laser. UV-VIS absorption spectra were collected in water and ethanol solutions by Perkin Elmer Lambda 750 in the spectral region of 200–900 nm.

### **2.1. Calculation Details**

Isomers of 6A2T5CA were analyzed using the B3LYP/6-311G(2d,2p) basis set in gas phase. Theoretical UV-VIS spectra were obtained using B3LYP/6-311G(2d,2p) method in the TD-DFT framework. Theoretical parameters of 6A2T5CA were calculated with Gaussian 09 [23]. GaussView 5.0.8 program was used to visualize of the chemical structure and vibrational spectra [24]. It was concluded that oxo isomer has lower energy than the hydroxyl isomer. Therefore, the experimental results were compared with oxo isomer of 6A2T5CA. Total energy distribution (TED) calculations were performed with scaled quantum mechanical (SQM) [25, 26]. In the SQM, the internal coordinates of all molecules are divided into some groups sharing a common scaling factor, and the factors for each group are defined by a least-squares fitting to experimentally obtained vibrational frequencies [25]. PED analysis allows quantitatively to describe the distribution of the motion of a given group of atoms. It is used to find the distribution of local mode energies in the overall energy of the normal mode [27].

## **3. RESULTS AND DISCUSSIONS**

### **3.1. Geometrical Structure**

Two different isomer forms of the title molecule were investigated in this study. Two different isomers of 6A2T5CA are shown in Fig. 1. All of the experimental results were compared with oxo isomer, because oxo isomer form of the title molecule has the lowest optimization energy. Moreover, some geometric parameters were computed and these computed parameters were compared with experimental results (Table 1). It was shown that there was an agreement between experimental and computed data.

Bond angles of C2-N7-C1, N7-C1-S and C1-N6-H4 were calculated as 119.993°, 119.993° and 120.011°, respectively. These values were given as 122.9, 122.2 and 121.0° in the literature [28]. Calculated C1-N6, N7-H5 and C1-S bond distances were found as 1.394, 1.091 and 1.680 Å. These values were founded as 1.389, 0.90 and 1.683 Å, respectively. Some geometric parameters of 6A2T5CA were shown in Table 2.

**Table 1.** Computed energy values and dipole moment values of title molecule by B3LYP/6-311G(2d,2p)

Conformers	Energy		Energy Differences		Dipol Moment (Debye)
	Hartree	Kcal/mol	Hartree	Kcal/mol	
Oxo	-942.30122921	-591303.07498831	0	0	1.2078
Hydroxy	-942.28367890	-591292.0620002	0.0175503	11.01298815	2.0654

**Table 2.** Some geometric parameters of 6A2T5CA

Parameters	Calculated	Experimental [16]
<b>Bond Lengths (Å)</b>		
C1-N6	1.394	1.389
N7-H5	1.091	0.90
N6-H4	1.091	0.90
C2-C3	1.395	1.432
C1-S	1.680	1.683
<b>Bond Angles (°)</b>		
C2-N7-C1	119.993	122.900
N7-C1-S	119.993	122.200
C1-N6-H4	120.011	121.000
C3-C2-N7	120.005	121.200
O9-C2-C3	119.983	125.000

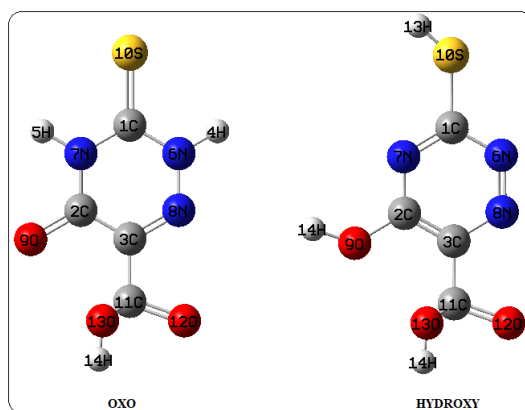


**Figure 1.** Possible isomer forms of the title molecule

Oxo and hydroxy forms following equations can be written for the mole fractions of individual conformers where a and b are oxo and hydroxyl, respectively:



$$K_T = \frac{N_b}{N_a} \quad \text{and} \quad N_a + N_b = 1$$

where  $K_T$  is conformational equilibrium constant between oxo and hydroxyl,  $N_a$  and  $N_b$  are mole fractions of conformers oxo and hydroxyl.

$$K_T = e^{-\Delta G/RT}, R=1987 \times 10^{-3} \text{ kcal/mol.K, } T = 298 \text{ K and } \delta\Delta G = \Delta G_b - \Delta G_a \text{ [29]}$$

The following mole fractions were obtained:  $N_a = 0.66$  and  $N_b = 0.34$ . Based on the calculations, the oxo form is the most stable and the most abundant conformer in the gas phase.

### 3.2. Vibrational Studies of 6A2T5CA

The vibrational frequencies, vibrational intensities and band assignments of the title molecule are given in Table 3. The experimental and calculated FT-IR and Raman spectra for the title molecule are given in Figures 2 and 3. Obtained experimental results were assigned to the theoretical results of oxo isomer of the title molecule.

Raman scattering activities were converted to Raman intensities using the given equation [30, 31]:

$$I_i = \frac{f(\nu_0 - \nu_i)^4 S_i}{\nu_i \left[ 1 - \exp\left(\frac{h c \nu_i}{k T}\right) \right]}$$

Here,  $\nu_0$  is the laser exciting wavenumber (in this study,  $\nu_0 = 18797 \text{ cm}^{-1}$ ),  $\nu_i$  the vibrational wavenumber of the  $i^{\text{th}}$  normal mode and  $S_i$  is the Raman scattering activity of the normal mode  $\nu_i$ ,  $f$  is a optional normalization factor for all peak intensities.  $h$ ,  $k$ ,  $c$  and  $T$  are Planck and Boltzmann constants, speed of light and temperature respectively.

#### 3.2.1. OH modes

The OH stretching band is observed range from  $3600$  to  $3400 \text{ cm}^{-1}$  and this band appears as a very broad band in the FT-IR spectrum. OH vibration bands show intra and inter molecular hydrogen bonding [32]. In this study, O–H stretching band was observed at  $3255 \text{ cm}^{-1}$  in the FT-IR spectrum, at  $3259 \text{ cm}^{-1}$  in the Raman spectrum and this band was calculated as  $3256 \text{ cm}^{-1}$ . Moreover, this mode is pure stretching mode because TED value of this mode was observed as 100% (Table 3). Both experimental and theoretical wavenumbers are an agreement with the literatures [33]. On the other hand, OH in-plane bending vibration was appeared at  $1016 \text{ cm}^{-1}$  in the FT-IR spectrum, at  $1002 \text{ cm}^{-1}$  in the Raman spectrum and calculated as  $1040 \text{ cm}^{-1}$ . OH out plane bending vibration was observed at  $592 \text{ cm}^{-1}$  in FT-IR spectrum,  $602 \text{ cm}^{-1}$  in the Raman spectrum and calculated as  $593 \text{ cm}^{-1}$ .

#### 3.2.2. NH modes

In general, NH stretching vibrations have low intensities and they are observed as weak signals in the both FT-IR and Raman spectra [34]. NH stretching vibrations of the title molecule were observed at  $3469$  and  $3423 \text{ cm}^{-1}$  in the IR spectrum and calculated as  $3468$  and  $3410 \text{ cm}^{-1}$ , respectively. The NH rocking mode in the FT-IR was found at  $1418 \text{ cm}^{-1}$ , and  $1422 \text{ cm}^{-1}$  in the Raman spectrum. This mode was calculated as  $1426 \text{ cm}^{-1}$ .

#### 3.2.3. CC modes

CC stretching vibrations of the aromatic ring are very crucial because they determine characteristic of the aromatic ring. In the literature, CC stretching vibrations are observed between  $1620$  and  $1320 \text{ cm}^{-1}$  in the FT-IR spectrum [35]. The experimental and computed IR and Raman spectra of 6A2T5CA are given in Figures 2 and 3. CC stretching vibrations of the title molecule were observed at  $1578 \text{ cm}^{-1}$  and  $1418 \text{ cm}^{-1}$  in the FT-IR spectrum. These vibrations were observed at  $1578$  and  $1422 \text{ cm}^{-1}$  in the Raman spectrum and calculated as  $1579$  and  $1426 \text{ cm}^{-1}$ , respectively. The C–C stretching vibrations are

generally pure modes because of their TED values. However, sometimes these modes can include other vibration modes. In this case, CC modes were contaminated by NH vibrations.

### 3.2.4. CN modes

The determination of CN vibrations is very difficult, because the area is contaminated with other vibration modes. In the literature, CN stretching modes are observed between 1295 and 1245  $\text{cm}^{-1}$  [36]. CN stretching vibrations of the title molecule were observed at 1270, 1164  $\text{cm}^{-1}$  in the FT-IR, at 1270 and 1176  $\text{cm}^{-1}$  in the Raman spectrum and calculated as 1247 and 1182  $\text{cm}^{-1}$ , respectively. These vibration wavenumbers are in agreement with the literature [37]. CN stretching modes and their TED values are collected in Table 3.

### 3.2.5. CO modes

The CO vibrations are usually observed at high intensity and therefore these vibrations are very easy to separate from other vibration modes. In the literature, C-O vibrations are observed between 1000-1300  $\text{cm}^{-1}$  and C=O vibrations are appeared in the range from 1750 and 1650  $\text{cm}^{-1}$  [38, 39]. C-O vibrations of title molecule were appeared at 1325 and 1016  $\text{cm}^{-1}$  in the FT-IR spectrum, at 1331 and 1002  $\text{cm}^{-1}$  in the Raman spectrum, these vibrations were calculated as 1334 and 1040  $\text{cm}^{-1}$ , respectively. C=O vibrations of title molecule were appeared at 1735 and 1685  $\text{cm}^{-1}$  in the FT-IR spectrum, at 1747 and 1690  $\text{cm}^{-1}$  in the Raman spectrum. These vibrations were calculated as 1736 and 1674  $\text{cm}^{-1}$ , respectively.

The correlation graphics between experimental and computed wavenumbers are shown in Fig. 4. It was observed that there was a good agreement between experimental and calculated wavenumbers.

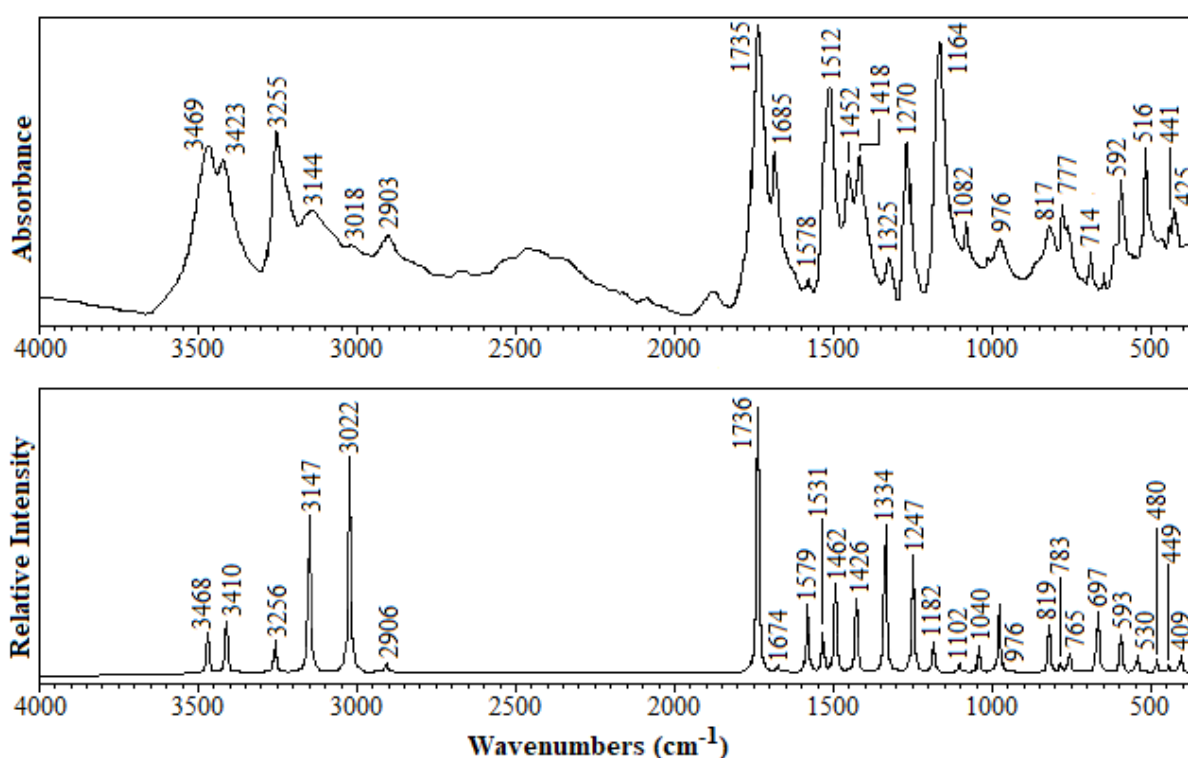


Figure 2. Experimental (up) and computed (down) FT-IR spectra of 6A2T5CA.

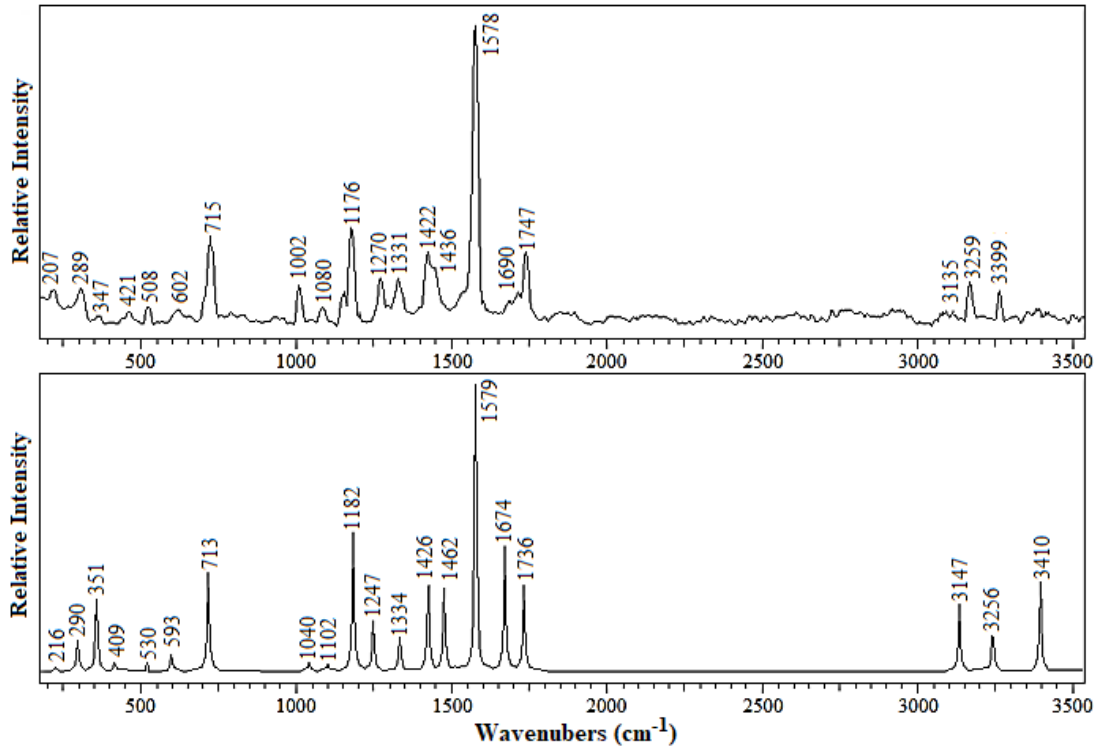


Figure 3. Experimental (up) and computed (down) Raman spectra of 6A2T5CA.

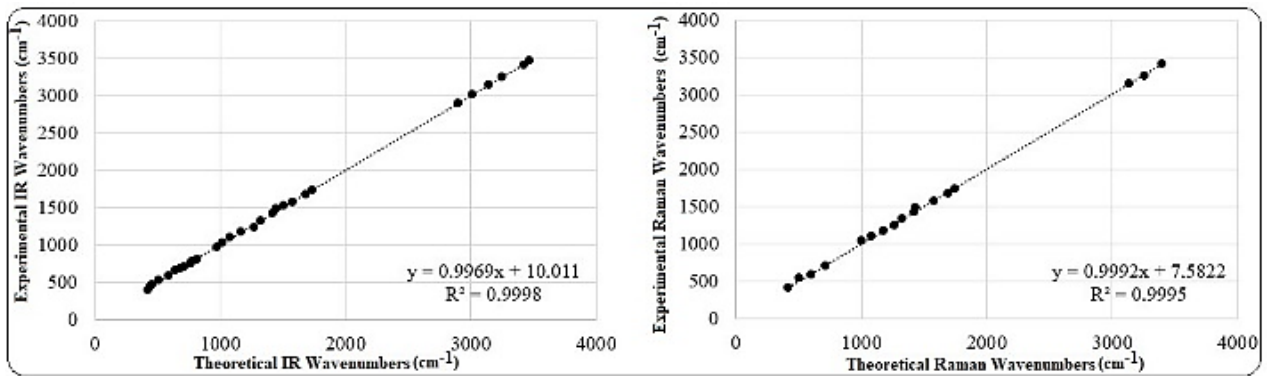


Figure 4. Plot of the experimental and theoretical wavenumbers 6A2T5CA.

**Table 3.** Comparison of the experimental and calculated vibrational wavenumbers (cm<sup>-1</sup>) of 6A2T5CA

Modes	Experimental Wavenumbers (cm <sup>-1</sup> )		Theoretical Wavenumbers (cm <sup>-1</sup> )				Assignments
	IR	Raman	6-311G(2d,2p)				
			Unscaled.	SQM	I <sub>IR</sub>	I <sub>R</sub>	
v <sub>1</sub>	3469	-	3647	3468	15.09	-	NH stretching (100)
v <sub>2</sub>	3423	3399	3586	3410	20.34	10.41	NH stretching (100)
v <sub>3</sub>	3255	3259	3348	3256	12.63	5.27	OH stretching (100)
v <sub>4</sub>	3144	3135	3309	3147	65.84	8.34	CH stretching (100)
v <sub>5</sub>	3018	-	3178	3022	91.93	-	CH stretching (98)
v <sub>6</sub>	2903	-	3056	2906	4.15	-	CH stretching (98)
v <sub>7</sub>	1735	1747	1825	1736	100	12.16	CO stretching (95)
v <sub>8</sub>	1685	1690	1714	1674	2.92	10.61	CO stretching (93)
v <sub>9</sub>	1578	1578	1611	1579	25.73	20.82	CC stretching (63) + CNH bending (26)
v <sub>10</sub>	1512	-	1598	1531	14.77	-	CN stretching (36) + CNN bending (18)
v <sub>11</sub>	1452	1436	1548	1462	33.28	11.89	CN stretching (38) + CNN bending (16) + CNH bending (13) + HCH wagging (18) + CH stretching (11)
v <sub>12</sub>	1418	1422	1460	1426	28.44	12.08	NH rocking (66) + CC stretching (12) + CNH bending (11) + HCH twisting (10)
v <sub>13</sub>	1325	1331	1366	1334	57.51	4.21	CO stretching (21) + COH bending (18)
v <sub>14</sub>	1270	1270	1277	1247	49.25	5.60	CN stretching (67) + CH deformation of ring
v <sub>15</sub>	1164	1176	1229	1182	12.63	11.27	NN stretching (54) + CN stretching (23) + COH bending (10)
v <sub>16</sub>	1082	1080	1128	1102	4.68	0.39	NN stretching (18) + COH bending (10)
v <sub>17</sub>	1016	1002	1065	1040	10.69	0.71	CN stretching (41) + CO stretching (30) + OH in plane bending (19)
v <sub>18</sub>	976	-	999	976	26.44	-	CS stretching (72)
v <sub>19</sub>	817	-	839	819	18.33	-	OH bending (58), CH bend of ring skeletal deformation
v <sub>20</sub>	777	-	802	783	16.29	-	OH bending (49), CH bending (11)
v <sub>21</sub>	764	-	778	765	9.09	-	CH in plane bending (29) + CH bending (24) + NH in plane bending (13)
v <sub>22</sub>	714	715	730	713	0.35	15.34	CCC bending (32)
v <sub>24</sub>	690	-	714	697	0.26	-	CC stretching (19) + OCO bending (17)
v <sub>25</sub>	647	-	681	665	26.56	-	CN stretching (27) + CS stretching (16) + NH bending (14) + COC wagging (10) + CH deformation of ring
v <sub>26</sub>	592	602	607	593	14.56	3.18	OCN bending (40) + NH bending (23) + HCH wagging (22) + OH out plane bending (13)
v <sub>28</sub>	516	508	563	530	7.28	1.96	Ring deformation
v <sub>29</sub>	462	-	492	480	5.15	-	CS stretching (24) + Ring deformation
v <sub>30</sub>	441	-	459	449	0.81	-	OH bending (22)
v <sub>31</sub>	425	421	419	409	0.96	4.27	Ring deformation
v <sub>32</sub>	-	347	359	351	-	2.08	HCH rocking (24) + OH bending (17)
v <sub>33</sub>	-	289	297	290	-	1.12	OH bending (12)
v <sub>34</sub>	-	207	221	216	-	0.43	CNN bending (19) + SCN bending (16)

Calculated and experimental vibrational were examined with root mean-square (RMS). RMS values were calculated by the following relationship [40];

$$\text{RMS} = \sqrt{\frac{1}{n-1} \sum_{i=1}^n (v_i^{\text{calc}} - v_i^{\text{exp}})^2}$$

RMS value for FT-IR wavenumbers was calculated as  $11.96\text{ cm}^{-1}$  and calculated as  $15.66\text{ cm}^{-1}$  for Raman vibration. Differences have been because of hydrogen bonds vibrations observed between the experimental and theoretical wavenumbers. These vibrations cause strong perturbation of other vibrational modes [41].

### 3.3. UV–VIS Spectrum

Experimental UV–VIS spectra of 6A2T5CA were collected at room temperature in water and ethanol. Moreover, theoretical UV–VIS spectrum was obtained using B3LYP/6-311G(2d,2p) method in the TD-DFT framework. Theoretical wavelengths ( $\lambda$ ), excitation energies (E), electronic transitions and experimental absorption wavelengths and energies are given in Table 4 in both water and ethanol. In addition, both experimental and theoretical UV–VIS spectra of title molecule were given in Fig. 5. Experimental values of maximum absorption are 213, 270 and 315 nm in water, 210, 271 and 317 nm in ethanol, respectively. Theoretical maximum absorption values were calculated as 209, 268 and 342 nm in water, 215, 269 and 332 nm in ethanol.

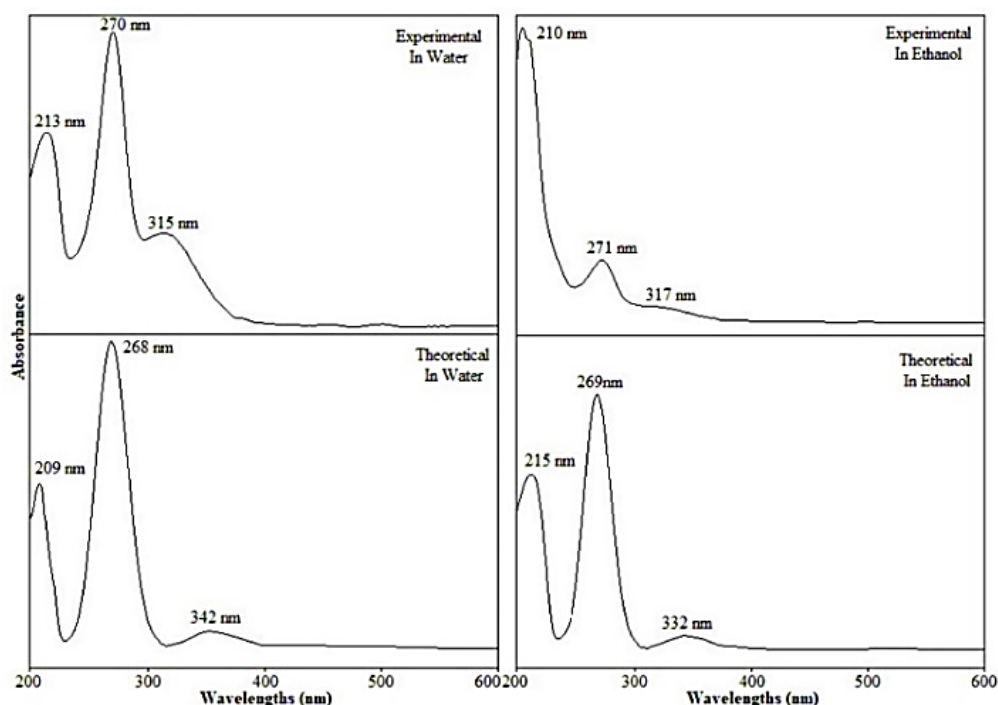


Figure 5. Experimental and theoretical UV–VIS spectra of 6A2T5CA in water and ethanol

Table 4. Experimental and calculated wavelengths ( $\lambda$ ), excitation energies, of 6A2T5KA in water and ethanol

$\lambda$ (nm)	E (eV)	Assignments	$\lambda$ (nm)	E (eV)
<b>B3LYP/6-311G(2d, 2p)</b>			<b>Experimental</b>	
In Water				
209	5.93226	$\pi \rightarrow \pi^*$	213	5.82085
268	4.62628	$\pi \rightarrow \pi^*$	270	4.59201
342	3.62527	$\pi \rightarrow \pi^*$	315	3.93601
In Ethanol				
215	5.7667	$\pi \rightarrow \pi^*$	215	5.7667
269	4.60908	$\pi \rightarrow \pi^*$	271	4.57506
332	3.73446	$\pi \rightarrow \pi^*$	317	3.91117

### 3.4. HOMO-LUMO Analysis

HOMO and LUMO are described as the highest occupied molecular orbital and lowest unoccupied molecular orbital, respectively [42]. HOMO, LUMO and HOMO-LUMO energy gaps have been performed with using DFT at B3LYP/6-311G(2d,2p) level of theory. The plots of HOMO and LUMO of the title molecule were given in Figure 5. Energy gap value of the title molecule was calculated as 3.790 eV. The nodes of HOMO orbital located on the sulfur, nitrogen and oxygen atoms. However, LUMO nodes were located symmetrically all over molecule. Also, charge of the sulfur atom shifted carbonyl group from HOMO to LUMO.

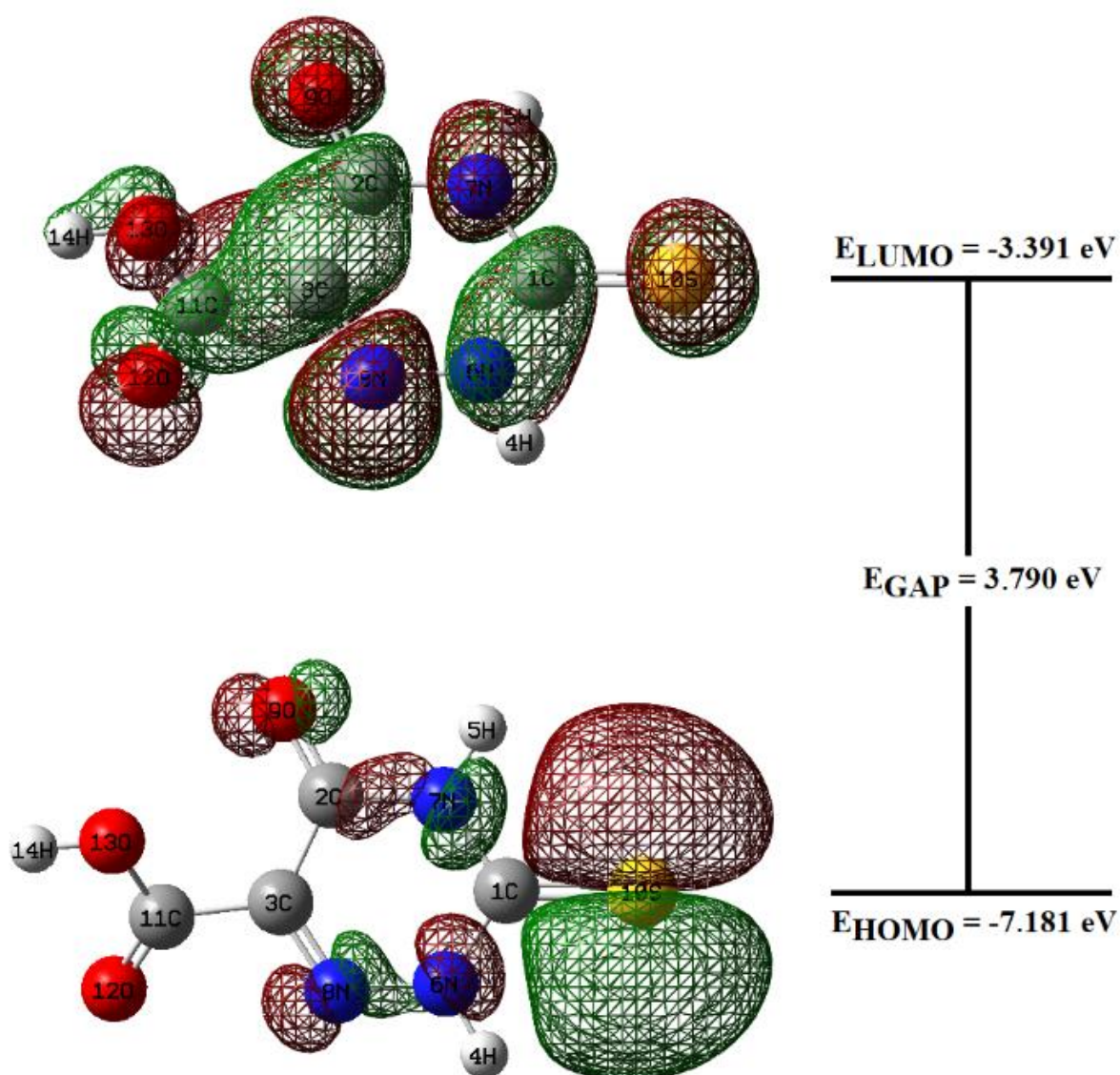


Figure 5. Frontier molecular orbitals of title molecule.

### 3.5. Molecular Electrostatic Potential (MEPs) of 6A2T5CA

The MEP gives information about chemical reactivity of a molecule. The values of electrostatic potential are shown by different colors (from blue to red) which increases from red color to blue. In addition, positive, negative and neutral electrostatic potential regions can be obtained by the MEP surface [43, 44]. The MEPs of the title molecule are given in Fig. 6. The MEPs map of the title molecule indicated that near oxygen atoms have negative potential.

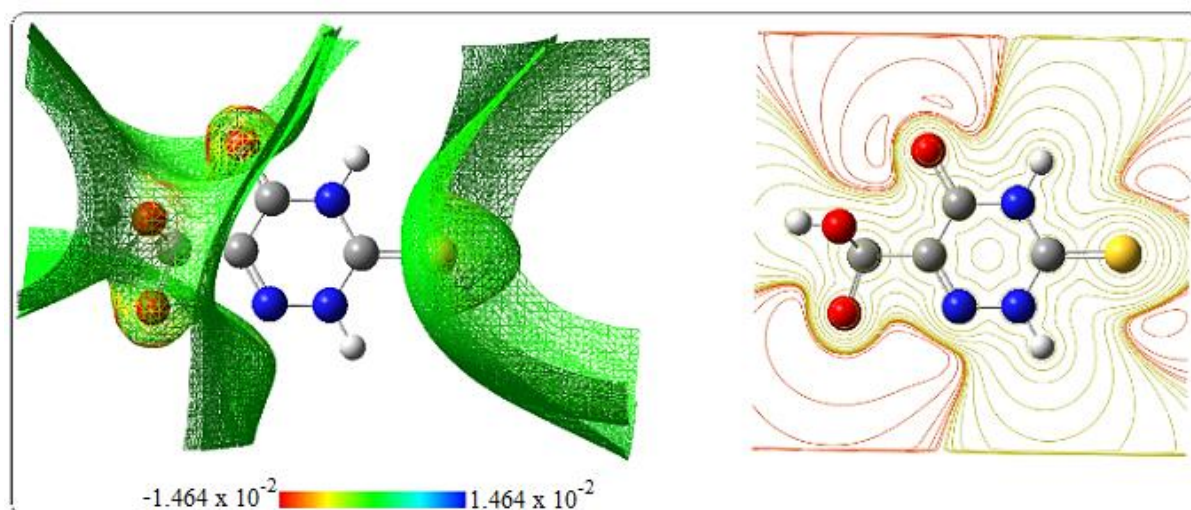


Figure 6. MEPs map of 6A2T5CA

## 4. CONCLUSION

In this study experimental IR and Raman spectra were obtained and theoretical IR and Raman spectra were analyzed using Gaussian 9.0 with B3LYP/6-311G(2d,2p) level of theory. Experimentally obtained wavenumbers of title molecule were compared with theoretically obtained wavenumbers. Two different isomers (oxo and hydroxyl) of the title molecule were examined and oxo isomer has the lowest optimized energy in the gas phase. It was observed that experimental and theoretical results were in alignment with each other. As a result, B3LYP/6-311G(2d, 2p) basis set can be used to investigation of vibrational and geometrical properties of the title molecule.

## ACKNOWLEDGEMENT

This study was supported by the Scientific Research Projects Commission of Eskişehir Osmangazi University: (Project no 201846014).

## CONFLICT OF INTEREST

The author stated that there are no conflicts of interest regarding the publication of this article.

## REFERENCES

- [1] Saenger W. Principles of Nucleic Acid Structure. Springer-Verlag, New York Berlin Heidelberg, Tokyo, 1984.
- [2] Beck CF, Howlett, G. The nature of the miscoding caused by growth in the presence of 2-thiouracil. *J Mol Biol* 1977; 111: 1-17.
- [3] Nei YW, Akinyemi, TE, Kaczan, CM, Steill, JD, Berden, G, Oomens, J, Rodgers, MT. Infrared multiple photon dissociation action spectroscopy of sodiated uracil and thiouracils: Effects of thio keto-substitution on gas-phase conformation. *Int J Mass Spectrom* 2011; 308(2–3): 191-202.
- [4] Gottschalk E, Kopp E, Lezius AG. A synthetic DNA with unusual base-pairing. *Eur J Biochem* 1971; 24: 168-182.
- [5] Bretner M, Kulikowski T, Dzik JM, Rode W, Shugar D. 2-Thio derivatives of dUrd and 5-fluoro-dUrd and their 5'-monophosphates: synthesis, interaction with tumor thymidylate synthase, and in vitro antitumor activity. *J Med Chem* 1993; 36: 3611-3617.
- [6] Beck CF, Howlett GJ. The nature of the miscoding caused by growth in the presence of 2-thiouracil. *J Mol Biol* 1977; 111: 1-17.
- [7] Kryachko ES, Nguyen MT, Zeeger-Huyskens T. Thiouracils: Acidity, Basicity, and Interaction with Water. *J Phys Chem A* 2001; 105: 3379-3387.
- [8] Moustafa H, El-Taher S, Shibl MF, Hilal R. Equilibrium Geometry and Gas-Phase Proton Affinity of 2-Thiouracil Derivatives. *Int J Quantum Chem* 2002; 87: 378–388.
- [9] Singh R, Jaiswal S, Kumar M, Singh P, Srivastav G, Yadav RA. DFT study of molecular geometries and vibrational characteristics of uracil and its thio-derivatives and their radical cations. *Spectrochim Acta A Mol Biomol Spectrosc* 2010; 75: 267-276.
- [10] Lapinski L, Prusinowska D, Nowak MJ, Bretner M, Felczak K, Maes G, Adamowicz L. Infrared spectra of 6-azathiouracils: an experimental matrix isolation and theoretical ab initio SCF/6-311G\*\* study. *Spectrochim Acta A Mol Biomol Spectrosc* 1996; 52: 645-659
- [11] Beranek J, Acton EM. Inhibition of nucleic acid synthesis in L1210 cells by nucleoside analogs. *Collect Czech Chem Commun* 1984; 49: 2551-2556.
- [12] Roche KL, Nukui M, Krishna BA, O'Connor CM, Murphy EA. Selective 4-thiouracil labeling of RNA transcripts within latently infected cells after infection with human cytomegalovirus expressing functional uracil phosphoribosyltransferase. *J Virol* 2018; 92: e00880-18 (1-16).
- [13] Alcolea Palafox M, Rastogi VK, Singh SP. Effect of the Sulphur Atom on Geometry and Spectra of the Biomolecule 2-Thiouracil and in the WC Base Pair 2-Thiouridine-Adenosine. Influence of water in the first hydration Shell. *J Biomol Struct Dyn* 2018; 36: 1225–1254.
- [14] Nishimura Y, Tshuboi M, Kato S, Morokuma K. In-Plane Vibrational Modes in the Uracil Molecule from an ab Initio MO Calculation. *J Am Chem Soc* 1981; 103: 1354-1358.

- [15] Yang W, Hu Y. Conformations of 2-thiouracil in the aqueous solution and its adsorption behavior on the gold substrates explored by DFT calculations and experimental methods. *Spectrochim. Acta A* 2015; 134: 399–405.
- [16] Zou X, Dai X, Liu K, Zhao H, Song D, Su H. Photophysical and photochemical properties of 4-thiouracil: Time-resolved IR spectroscopy and DFT studies. *J Phys Chem B* 2014; 118: 5864–5872.
- [17] Prasanthkumar KP, Suresh CH Aravindakumar CT. Dimer radical cation of 4-thiouracil: A pulse radiolysis and theoretical study. *J Phys Org Chem* 2013; 26: 510–516.
- [18] Shukla MK, Leszczynski J. A theoretical study of hydration of 4-thiouracil in the electronic singlet excited state. *J Mol Struct* 2006; 771: 149–155.
- [19] Li YS, Jalilian MR, Durig JR. Microwave spectrum of indene. *J Mol Struct* 1979; 51: 171-174.
- [20] Yan J, Jin S, Wang B. A novel redox-sensitive protecting group for boronic acids, MPMP-diol. *Tetrahedron Lett* 2005; 46: 8503-8505.
- [21] Rauhut G, Pulay P. Transferable Scaling Factors for Density Functional Derived Vibrational Force Fields. *J Phys Chem* 1995; 99: 3093-3100.
- [22] Lee SY. Molecular Structure and Vibrational Spectra of Biphenyl in the Ground and the Lowest Triplet States. Density Functional Theory Study. *B Korean Chem Soc* 1998; 19(1): 93-98.
- [23] Frisch MJ, *et al.* Gaussian 09, Revision A. 1, Gaussian, Inc, Wallingford, CT. 2009.
- [24] Dennington R, Keith T, Millam J. GaussView, Version 5.0 Semichem Inc., KS (2005)
- [25] Rauhut G, Pulay P. Transferable scaling factors for density functional derived vibrational force fields. *J Phys Chem* 1995; 99: 3093-3100.
- [26] Baker J, Jarzecki AA, Pulay P. Direct scaling of primitive valence force Constants: an alternative approach to scaled quantum mechanical force fields. *J Phys Chem A* 1998; 102: 1412-1414.
- [27] Jamroz MH. Vibrational Energy Distribution Analysis (VEDA): Scopes and limitations. *Spectrochim Acta A Mol* 2013; 114: 220-230.
- [28] Tiekink ERT. Crystal structure of 2-thiouracil. *Z Kristallogr* 1989; 187: 79-84.
- [29] Hür D, Güven A. The acidities of some indoles. *J Mol Struct Theochem* 2002; 583 (1–3): 1-8.
- [30] Keresztury G, Holly S, Varga J, Besenyi G, Wang AY, Durig JR. Vibrational spectra of monothiocarbamates-II. IR and Raman spectra, vibrational assignment, conformational analysis and ab initio calculations of S-methyl-N, N-dimethylthiocarbamate. *Spectrochim Acta A* 1993; 49A: 2007-2026.
- [31] Keresztury G. Raman spectroscopy: theory, J.M. Chalmers, P.R. Griffith (Eds.), *Handbook of Vibrational Spectroscopy*, vol. 1, John Wiley & Sons Ltd., New York, 2002, 71-87.
- [32] Stuart B. *Infrared Spectroscopy: Fundamentals and Applications*. Wiley India Ed. 2010.

- [33] Dikmen G. 4-Methyl-1H-Indazole-5-Boronic acid: Crystal structure, vibrational spectra and DFT simulations. *J Mol Struct* 2017; 1150: 299-306.
- [34] Oomens J, Meijer G, Helden GV. An infrared spectroscopic study of protonated and cationic indazole. *Int J Mass Spectrom* 2006; 249–250: 199-205
- [35] Dikmen G, Alver Ö. NMR, FT-IR, Raman and UV–Vis spectroscopic investigation and DFT study of 6-Bromo-3-Pyridinyl Boronic Acid. *J Mol Struct* 2015; 1099: 625-632.
- [36] Li Y, Liu Y, Wang H, Xiong X, Wei P, Li F. Synthesis, Crystal Structure, Vibration Spectral, and DFT Studies of 4-Aminoantipyrine and Its Derivatives. *Molecules* 2013; 18: 877-893.
- [37] Seshadri S, Gunasekaran S, Muthu S. Vibrational spectroscopy investigation using density functional theory on 7-chloro-3-methyl-2H-1,2,4- benzothiadiazine 1,1-dioxide. *J Raman Spectrosc* 2009; 40: 639-644.
- [38] Solaichamya R, Karpagama J. Structural and Vibrational studies (FT-IR, FT-Raman) of Voglibose using DFT calculation. *ILCPA* 2016; 64: 45-62.
- [39] Puviarasan N, Arjunan V, Mohan S. FT-IR and FT-Raman Studies on 3-Aminophthalhydrazide and N-Aminophthalimide. *Turk J Chem* 2002; 26: 323-333.
- [40] Teimouri A, Chermahini AN, Tabanc K, Dabbagh HA. Experimental and CIS, TD-DFT, ab initio calculations of visible spectra and the vibrational frequencies of sulfonyl azide-azoic dyes. *Spectrochim Acta A* 2009; 72: 369-377
- [41] Sapic IM, Bisticic L, Volovseka V, Dananic V, Furic K. DFT study of molecular structure and vibrations of 3-glycidoxypropyltrimethoxysilane. *Spectrochim. Acta A* 2009; 72: 833-840
- [42] Rajesh SP, Gunasekaran T, Gnanasambandan, SS. Molecular structure and vibrational analysis of Trifluoperazine by FT-IR, FT-Raman and UV–Vis spectroscopies combined with DFT calculations. *Spectrochim Acta A*: 2015; 137: 1184-1193.
- [43] Kosov DS, Popelier, PLA. Atomic Partitioning of Molecular Electrostatic Potentials. *J Phys Chem A* 2000; 104: 7339-7345.
- [44] Suvitha A, Periandy S, Gayathri P. NBO, HOMO–LUMO, UV, NLO, NMR and vibrational analysis of veratrole using FT-IR, FT-Raman, FT-NMR spectra and HF–DFT computational methods. *Spectrochim Acta A*: 2015; 138: 357-369.